Interaction of Pure Marangoni Convection with a Propagating Reactive Interface under Microgravity

P. Bába
Department of Physical Chemistry and Materials Science, University of Szeged, Aradi vértanúk tere 1, Szeged H-6720, Hungary

L. Rongy
Nonlinear Physical Chemistry Unit, Université libre de Bruxelles (ULB), Campus Plaine, C.P. 231, 1050 Brussels, Belgium

A. De Wit
Nonlinear Physical Chemistry Unit, Université libre de Bruxelles (ULB), Campus Plaine, C.P. 231, 1050 Brussels, Belgium

M. J. B. Hauser
Institute of Biometry and Medical Informatics, Otto von Guericke Universität Magdeburg, Leipziger Straße 44, D-39120 Magdeburg, Germany and Institute of Physics, Otto von Guericke-Universität Magdeburg, Universitätsplatz 2, D-39106 Magdeburg, Germany

Á. Tóth
Department of Physical Chemistry and Materials Science, University of Szeged, Aradi vértanúk tere 1, Szeged H-6720, Hungary

D. Horváth*
Department of Applied and Environmental Chemistry, University of Szeged, Rerrich Béla tér 1, Szeged H-6720, Hungary

(Received 30 October 2017; revised manuscript received 30 January 2018; published 9 July 2018)

A reactive interface in the form of an autocatalytic reaction front propagating in a bulk phase can generate a dynamic contact line upon reaching the free surface when a surface tension gradient builds up due to the change in chemical composition. Experiments in microgravity evidence the existence of a self-organized autonomous and localized coupling of a pure Marangoni flow along the surface with the reaction in the bulk. This dynamics results from the advancement of the contact line at the surface that acts as a moving source of the reaction, leading to the reorientation of the front propagation. Microgravity conditions allow one to isolate the transition regime during which the surface propagation is enhanced, whereas diffusion remains the main mode of transport in the bulk with negligible convective mixing, a regime typically concealed on Earth because of buoyancy-driven convection.

DOI: 10.1103/PhysRevLett.121.024501

The dynamics of reacting systems is usually studied under bulk or volume phase conditions, whereas any changes occurring at the boundaries between phases are often neglected, as the surface to volume ratio of the bulk phase is usually small. Considerable scientific attention has been devoted to systems in which the variations in physical parameters due to an autocatalytic reaction front [1], the self-organized location where reactants are transformed into products, give rise to hydrodynamic flows [2,3]. In particular, the interplay between reaction and convective motions induced by density changes brought about by the reaction has been extensively investigated [4–7]. The reaction-induced convective fluid flows then couple back with the reaction front, thus affecting the front velocity and shape [8–14]. In such reaction-diffusion-convection systems, studied both experimentally [15–17] and numerically [10,18–22], the reaction front is the only relevant interface.

By contrast, in many situations, an additional interface, the one between the liquid layer and the atmosphere, may frequently become important. These surfaces behave actively if the reaction creates a gradient in surface tension that leads to surface flows, and hence to surface-tension-driven or Marangoni convection, resulting in accelerating chemical waves [7], affecting precipitate patterns behind a chemical front [2], causing a switch between reactive states in a three-dimensional chemical wave [13], and modifying convection rolls that drive horizontally propagating fronts [17,23]. Marangoni flows can become important in a

number of scenarios, especially in the submillimeter range. They have been shown to lead to self-propulsion of droplets [24–26], pulsatory patterns in active fluids [27], interactions between active particles [28,29], and to continuous mixing of suspended materials [30]. The Marangoni shear stress, which can also arise upon contact of the reaction front propagating in the bulk liquid phase with the open liquid surface, can couple to the buoyant forces leading to intricate flow patterns [31]. The dynamics depends on the relative magnitude of surface tension versus buoyancy effects generally quantified by the Marangoni and Rayleigh numbers, respectively [31–35]. For a positive Marangoni number, defined as

$$\mathrm{Ma} = -\frac{\Delta\gamma}{\mu v_c}, \tag{1}$$

where $\Delta\gamma$ is the surface tension difference between the product and reactant solutions, μ the dynamic viscosity, and v_c the characteristic velocity, the surface-tension-induced convection leads to an advancement of the front at the interface, which is generally attributed to the underlying convection roll that transports the reaction intermediates farther away into the unreacted medium at the interface. This leads to an acceleration of the front.

In this Letter, we show that, in the absence of buoyancy, the coupling of Marangoni flow with a reactive interface in the bulk drives the onset of a self-organized localized vortex. It results from the Marangoni-enhanced advancement of the contact line, along which the reaction front meets the open surface, that acts as a moving reaction source. Generally, pure surface-tension-induced convection can hardly be isolated in macroscopic reactive systems when experiments are run on Earth since its contribution is often masked by much more pronounced convective flows stemming from density gradients. However, microgravity conditions produced in a sounding rocket eliminate density-induced effects, thus providing an experimental platform for the investigation of the effect of pure Marangoni flows on a propagating reactive interface. The results of the experimental studies are also compared with those of the numerical simulations based on computational fluid dynamics.

The iodate–arsenous-acid (IAA) reaction has become a prototype for studying reaction-induced convection in the presence of Marangoni flows since small changes in the initial concentrations may induce more or less pronounced buoyancy- and surface-tension-driven convective flow [10,21,36]. With reactant concentrations of potassium iodate $[KIO_3]_0 = 12.9$ mmol/l and arsenous acid $[H_3AsO_3]_0 = 36.1$ mmol/l, this yields a stoichiometry according to

$$5IO_3^- + 14H_3AsO_3 \rightarrow 2I^- + I_3^- + 14H_2AsO_4^- + 12H^+ + H_2O, \tag{2}$$

where iodide (I^-) and triiodide (I_3^-) are the main products besides arsenic acid (H_3AsO_4) [16]. Molecular iodine (I_2) is also present via the fast equilibrium $I_3^- \rightleftharpoons I_2 + I^-$. Since I_2 is the only surface-active species in the reaction medium, the surface tension of the product mixture is decreased with respect to that of the reactant solution [16]. In an unbuffered system, the reaction in Eq. (2) is autocatalytic in both iodide and hydrogen ions; therefore, the reaction occurs only at a negligible rate in a neutral or slightly basic solution [37].

Microgravity was achieved on board the European Space Agency sounding rocket MASER 13, launched from the Esrange Space Center, Sweden. The rocket reached its apogee at 259 km, providing 5 min 59 s of microgravity with an acceleration value of $g = (1.2 \pm 0.8) \times 10^{-3}$ m/s^2.

The premixed reactants were injected through bottom inlets into two quartz cells with identical length (x axis, 75 mm) and height (z axis, 15 mm) but a different width (y axis, 5 and 10 mm). The cells had an inner rim, the edge of which pinned the flat surface of the liquid layer, thus creating a 10-mm-deep layer of reaction solution that was in contact with a 5-mm-deep layer of air [38]. The reaction was then initiated by applying a 5 V potential difference for 4 s between two platinum wires (1 mm in diameter, with a spacing of 2 mm) located close to one lateral end of the cell and oriented along its z axis.

The spatiotemporal evolution of the propagating reaction front was monitored by a monochrome CCD camera using Fourier deflectometry with a blue backlight with a diagonal double fringe pattern. Gray scale images of 1920×640 pixels were recorded at 30 frames/s. The carrier frequency related to the fringe pattern was first subtracted from the Fourier spectra of the images and, by applying an inverse FFT, the amplitude maps represented the front images without the fringe pattern [39]. The front position was obtained for each image by locating the points of inflection in the x direction.

Particle image velocimetry (PIV) was used to monitor the convective motions of the fluid [40]. To do so, spherical latex beads with a diameter of 6.4 μm were dispersed in the potassium iodate solution to produce a particle density of 36 μg/cm^3 in the reaction cell. Vertical red laser sheets ($\lambda = 660$ nm), one positioned in the center x-z plane and two ± 1.5 mm apart, i.e., parallel to the longitudinal axis of the cells, were switched on and off alternatingly and gray scale images were recorded with 30 frames/s for each cell. The flow velocity vector field was then calculated by determining the spatial correlation between interrogation windows of 64×64 pixels for successive images. Particle tracking velocimetry (PTV) of individual tracer particles was also utilized on the same image set in order to determine the flow velocity close to the fluid-gas interface [41].

Upon electrochemical initiation of the front at a lateral wall of the cell, the solution quickly turns yellow at the anode due to the formation of triiodide in the acidic product mixture. The reaction front separating the reactant and the product solutions first spreads out from the vertical wire to fill the entire width of the cell, then continues to propagate along the long x axis. From the side view of the cell presented in

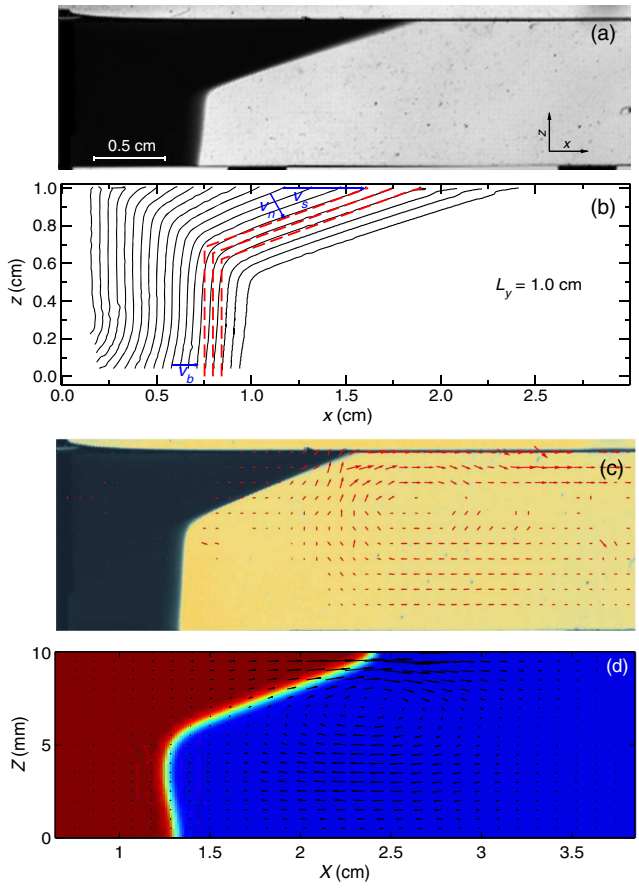

FIG. 1. (a) Side view of the 10-mm-wide cell at 317 s after initiation of the reaction. This corresponds to the end of the microgravity period. The dark region indicates the product solution containing triiodide behind the reaction front propagating from left to right. (b) Temporal evolution of the reaction front in the 10-mm-wide cell. The time delay between neighboring front profiles is 14.85 s. The red dashed lines are the reconstructed front profiles based on the geometric spreading of a RD front with the contact line advancing at a greater velocity on the free surface. Blue arrows indicate the displacement directions, along which the appropriate values for the velocity of propagation have been determined. Flow field in the center y-z plane of the cell superimposed over the false colored concentration field (c) in the experiment and (d) in the simulation. The measured fluid velocity in the bulk was obtained via PIV.

Fig. 1(a), the leading edge of the reaction front in the center x-z plane can be determined. Temporal monitoring of the front evolution reveals that the initially vertical reaction front soon becomes tilted at the surface [38] since the velocity of propagation is greater along the gas-liquid interface, as shown in Fig. 1(b). Furthermore, the monitoring of the surface also reveals that the reaction front does not cause any deformation of the liquid-air surface.

Following a transient period during which the front leaves the vicinity of the electrodes, the velocity takes on a constant value on the timescale of the experiment. At the surface, the front reaches a velocity $v_s = (5.72 \pm 0.05)$ mm/ min in the wider cell, which is 3 times larger than the observed $v_b = (1.81 \pm 0.02)$ mm/ min deep in the bulk and at the bottom. The latter is slightly slower than the velocity of a pure reaction-diffusion (RD) front in the IAA reaction, measured as (1.93 ± 0.02) mm/ min. The normal velocity of the tilted straight segment connecting the vertical part to the leading contact line on the surface is measured as $v_n = (1.95 \pm 0.02)$ mm/ min. This value falls in the range of that of the RD front velocity.

The velocity of propagation at the surface is ~20% of that of the same system under gravity [16], which results in a fivefold increase in the Marangoni number from 20 000 [16] to 100 000, with $\mu = 0.89$ mPa s and $v_c = v_s$, i.e., the front velocity at the surface. Here, we relate surface forces to viscous forces in the presence of a reaction front analogously to the traditional definition in the nonreactive case. The decrease in surface tension ($\Delta\gamma = -9.2$ mN/m) is due to the changes in composition since the thermal contribution is negligible, with the temperature increase well below 1 K in the vicinity of the front [16].

Smaller fluid velocity is observed at the surface in the narrower cell, indicating a larger dampening effect of the sidewalls in the y direction. Therefore, we conclude that there is a dominating effect of advective transport at the gas-liquid interface rather than diffusion of iodine in the gas phase, with the latter being eliminated by setting the reactant ratio to 2.8 [16].

In the bulk, the planar geometry of the vertical and tilted front segments and their normal velocity close to that of the RD fronts indicate that no significant fluid flow is present across the front. This scenario is supported by considering the geometric spreading of an initially vertical straight line with RD velocity and a moving point source on the top. The construction of isotemporal contour lines using the experimentally determined velocities maps out the front profiles [superimposed with red dashed lines in Fig. 1(b)], and hence confirms the negligible contribution of the fluid flow in the bulk. In other words, in the bulk, diffusion is the main mechanism of transport to be active around the front.

The velocity flow field in the center x-z plane obtained by PIV measurements demonstrates that, close to the accelerated tip at the surface, a large asymmetric convection roll develops around the reaction front. At the surface, it rotates in the same direction as the surface spreading of the product iodine, inducing a clockwise rotating convection roll [Fig. 1(c)]. However, its return flow due to continuity is too weak to significantly distort the reaction front in the bulk. With flow velocities well below that of the pure RD front, it causes only a small decrease in the propagation velocity of the vertical front segment.

In order to quantitatively describe the unexpected large velocity gradient in the vicinity of the surface, we have tracked the motion of individual tracer particles. These data show that the particles near the surface begin to move soon after the initiation of the reaction, with increasing velocity

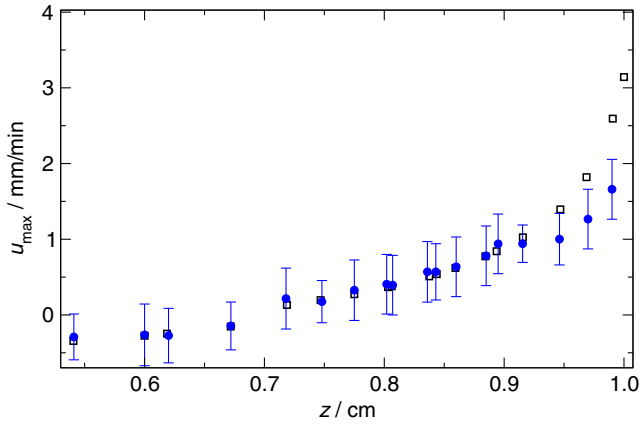

FIG. 2. Comparison of the maximum horizontal fluid motion velocity u_{max} as a function of the depth along the vertical center line of the 10-mm-wide cell. Here, the gas-liquid interface is located at $z = 1.0$ cm. The depth-dependent maximum fluid flow velocity u_{max} (full circles) was determined via PTV for particles in the proximity of the surface. Also, shown with black squares are the results of the model calculation for $M = 2$ rescaled to the appropriate dimensional coordinates with $l_c = 0.125$ mm and $t_c = 2.8$ s [1,32]. u_{max} is defined as the horizontal velocity with maximum absolute value; negative values of u_{max} hence corresponding to horizontal velocities directed to the left of the system.

followed by a rapid deceleration. The horizontal displacement and the velocity profile of the particles at the same depth are independent of the initial position along the long axis.

The maximum velocity reached in the similarly shaped velocity profiles of the individual particles strongly depend on the vertical position of the particle. The nonuniform distribution of the maximum horizontal velocity u_{max} within 5 mm adjacent to the gas-liquid interface is shown in Fig. 2. The measured velocity values rapidly decrease with increasing depth; within 1 mm of the surface the velocity reduces by more than half, while at a depth of 2.5 mm the drop in velocity reaches an order of magnitude. The inversion of the fluid flow is observed at 3.1–3.2 mm depth, below which the magnitude of the velocity does not exceed the value of 0.29 mm/ min. This latter value is 15% of the RD front velocity.

To support the experimental results, we model a two-dimensional thin reactive solution layer in contact with air [32]. In analogy with the experimental observations, we suppose no surface deformation and neglect any evaporation into the gas phase. The kinetics of the IAA reaction is accurately described by a four-variable model that can be further reduced to a one-variable cubic expression [42–44], where the only chemical variable is the concentration of the autocatalytic product that we set to be surface active. The propagation of the chemical front in the solution is described by numerically integrating the reaction-diffusion-convection equations governing the evolution of the concentration of the autocatalytic product coupled to the incompressible Navier-Stokes equations characterizing the flow field dynamics as [32]

$$\frac{\partial c}{\partial t} + \underline{v} \cdot \nabla c = \nabla^2 c + c^2(1-c), \tag{3}$$

$$\frac{\partial \underline{v}}{\partial t} + \underline{v} \cdot \nabla \underline{v} = S_c(-\nabla p + \nabla^2 \underline{v}), \tag{4}$$

$$\nabla \cdot \underline{v} = 0, \tag{5}$$

where we use dimensionless space and time coordinates scaled by the diffusional length (l_c) and chemical characteristic time (t_c), respectively. The dimensionless concentration c of the autocatalytic product is expressed relative to the initial concentration of the iodate reactant, $\underline{v} = (u, w)$ is the two-dimensional fluid velocity vector, $S_c = \nu/D$ is the Schmidt number with diffusion coefficient $D = 2.0 \times 10^{-9}$ m^2/s and kinematic viscosity $\nu = 1.0 \times 10^{-6}$ m^2/s.

We impose zero-flux boundary conditions for the chemical concentration c at the three solid boundaries of the system and at the gas-liquid surface, i.e., the free surface. The hydrodynamic boundary conditions at the rigid boundaries are no-slip conditions, $u = 0$ and $w = 0$. At the free surface we impose $w = 0$ since the surface is considered nondeformable, and we use a Marangoni boundary condition for the horizontal fluid velocity u, i.e., the velocity parallel to the x axis, to describe the changes in surface tension induced by the concentration gradient of the surface-active product across the front [45] according to

$$\frac{\partial u}{\partial z} = -M \frac{\partial c}{\partial x}, \tag{6}$$

where $M = -(d\gamma/dc)/(\mu l_c/t_c)$, with γ being the dimensional surface tension of the solution [32]. We note that if $d\gamma/dc$ could be approximated by $\Delta\gamma/\Delta c$, we would recover the experimental definition of the Marangoni number $\mathrm{Ma} \sim 10^5$ [Eq. (1)] since c is dimensionless and varies between 0 and 1. However, the experimental measurements of surface tension are equilibrium measurements that cannot accurately represent the local instantaneous variation of surface tension during the propagation of the front [16]. Indeed, there are two characteristic times, the one of the front propagation, t_c, which is relevant to the dynamics observed here, and an unknown relaxing time during which γ evolves to its equilibrium value at a fixed composition. In addition, we model a two-dimensional layer, and in the absence of the drag force of the sidewall, M is considered as an adjustable parameter. By comparing the numerical values of u_{max} to the experimental ones, the value of $M = 2$ has been measured (see Fig. 2). The use of Marangoni numbers smaller than the experimental is common in simplified models [23,32,35].

The initial condition corresponds to the reactant solution ($c = 0$) everywhere except in the first 0.5 cm on the left of the rectangular channel, where $c = 1$ to mimic the electrochemical initiation of the front with no fluid flow. Hence, the initial fluid velocity and the hydrostatic pressure gradient are zero everywhere in the system, and we use a steplike function for c. The equations are numerically integrated following a semi-implicit method [32].

Previous experimental and numerical results with chemically induced convection around chemical fronts evidenced the existence of an asymptotic regime attained at long times where the front propagates at a constant speed and with a stationary shape, surrounded by a steady convection roll [16,31]. This steady regime is observed on Earth where buoyancy-driven convection has a strong influence, whereas the results presented here describe the evolution of the transition regime.

The numerical simulations of the interaction of the flow dynamics with the autocatalytic chemical reaction described by Eqs. (3)–(5) reproduce the deformation of the originally straight reaction front oriented along the z axis [38]. The velocity gradient governed by the Marangoni boundary condition (6) generates an asymmetric convection roll, yet it has only a minor contribution to the distortion of the reaction front profile, in agreement with the experimental results [see Fig. 1(d)]. The Marangoni effect is also localized at the surface since the modeled horizontal velocity $u_{\max}$ significantly decreases away from the gas-liquid interface as shown in Fig. 2.

In this Letter, by conducting experiments in the absence of gravity, we have revealed that the Marangoni flow governed by a reaction-driven surface tension gradient acting along the open surface is localized at the region where the reaction front is in contact with the air-liquid interface. In this system the tip of the propagating reaction front at the surface forms a dynamic contact line where the gradient in surface tension is maximum due to the change in composition. The force along the surface generates a flow which is only significant in the reaction zone within 1 mm adjacent to the gas-liquid interface. The experiments also demonstrate that the contact line acts as a source for the reaction advancing along the surface, from which a RD front propagates to the bulk of the solution, with its leading edge comprising linear segments. The return flow of the single convection roll is shown to provide only a negligible contribution over the chemical timescale since it results in only a few percent (6%) decrease in the velocity of the vertical segment in the bulk without significantly distorting the geometry of the front such that the tilted segment advances basically with the velocity of a RD front. This morphology is drastically different from the one previously reported on Earth at the steady state. Owing to weak convection in the bulk, the fluid motion can be approximated by a two-dimensional flow field. Hence, a two-dimensional model simulation based on the Navier-Stokes equation coupled to the reaction kinetics can capture the general behavior of the reaction front. In general, the main effect of Marangoni flows on a reactive interface in the bulk is the reorientation of the propagation of the RD front. Unlike under gravity, no significant mixing of the reactants and products takes place, as the asymmetric convection roll arising at the reactive interface scales with the liquid depth. This mixing can become important only when the liquid layer is thin, i.e., when the drag force pointing in the opposite direction at the bottom interface is in the vicinity of the Marangoni force at the top liquid-air interface.

We gratefully acknowledge O. Minster, A. Verga, and B. Tóth (European Space Agency) for their contribution to the CDIC-3 project in the MASER 13 mission. We also thank K. Eckert (Technical University of Dresden) for helping the CDIC-3 project with her experience and useful comments, and E. Tóth-Szeles (University of Szeged) for her work during the module test phase and the flight mission. Fruitful discussions with V. Pimienta (University of Toulouse) and M. Budroni (University of Sassari) are acknowledged. We acknowledge the industrial contribution of Lambda-X S. A. (Nivelles, Belgium), Techno System Developments S.r.l. (Pozzuoli, Italy), DTM Technologies (Modena, Italy), and the Swedish Space Corporation (Solna, Sweden). The work was financially supported by European Space Agency (Grant No. ESTEC/4000102255/11/NL/KLM) and National Research, Development and Innovation Office (Grant No. K119795) and PROgramme de Développement d'Expériences scientifiques (Grant No. PEA40000104281).

*horvathd@chem.u-szeged.hu

[1] T. A. Gribschaw, K. Showalter, D. L. Banville, and I. R. Epstein, J. Phys. Chem. **85**, 2152 (1981).
[2] M. J. B. Hauser and R. H. Simoyi, Phys. Lett. A **191**, 31 (1994).
[3] I. R. Epstein and J. A. Pojman, *An Introduction to Nonlinear Dynamics: Oscillations, Waves, Pattern, and Chaos* (Oxford University Press, Oxford, 1998).
[4] G. Bazsa and I. R. Epstein, J. Phys. Chem. **89**, 3050 (1985).
[5] I. Nagypál, G. Bazsa, and I. R. Epstein, J. Am. Chem. Soc. **108**, 3635 (1986).
[6] J. A. Pojman and I. R. Epstein, J. Phys. Chem. **94**, 4966 (1990).
[7] H. Miike, H. Yamamoto, S. Kai, and S. C. Müller, Phys. Rev. E **48**, R1627 (1993).
[8] O. Inomoto, T. Ariyoshi, S. Inanaga, and S. Kai, J. Phys. Soc. Jpn. **64**, 3602 (1995).
[9] K. Matthiessen, H. Wilke, and S. C. Müller, Phys. Rev. E **53**, 6056 (1996).
[10] A. De Wit, Phys. Rev. Lett. **87**, 054502 (2001).
[11] I. Bou Malham, N. Jarrige, J. Martin, N. Rakotomalala, L. Talon, and D. Salin, J. Chem. Phys. **133**, 244505 (2010).
[12] É. Pópity-Tóth, D. Horváth, and Á. Tóth, J. Chem. Phys. **135**, 074506 (2011).

[13] L. Šebestíková and M. J. B. Hauser, Phys. Rev. E **85**, 036303 (2012).
[14] F. Rossi, M. A. Budroni, N. Marchettini, and J. Carballido-Landeira, Chaos **22**, 037109 (2012).
[15] G. Schuszter, T. Tóth, D. Horváth, and Á. Tóth, Phys. Rev. E **79**, 016216 (2009).
[16] É. Pópity-Tóth, V. Pimienta, D. Horváth, and Á. Tóth, J. Chem. Phys. **139**, 164707 (2013).
[17] D. Horváth, M. A. Budroni, P. Bába, L. Rongy, A. De Wit, K. Eckert, M. J. B. Hauser, and Á. Tóth, Phys. Chem. Chem. Phys. **16**, 26279 (2014).
[18] D. A. Vasquez, J. M. Littley, J. W. Wilder, and B. F. Edwards, Phys. Rev. E **50**, 280 (1994).
[19] A. De Wit, Phys. Fluids **16**, 163 (2004).
[20] L. Rongy, N. Goyal, E. Meiburg, and A. De Wit, J. Chem. Phys. **127**, 114710 (2007).
[21] J. Martin, N. Rakotomalala, L. Talon, and D. Salin, Phys. Rev. E **80**, 055101(R) (2009).
[22] N. Jarrige, I. Bou Malham, J. Martin, N. Rakotomalala, D. Salin, and L. Talon, Phys. Rev. E **81**, 066311 (2010).
[23] R. Guzman and D. A. Vasquez, Chaos **27**, 103121 (2017).
[24] K. Nagai, Y. Sumino, and K. Yoshikawa, Colloids Surf. B **56**, 197 (2007).
[25] Y.-J. Chen, Y. Nagamine, and K. Yoshikawa, Phys. Rev. E **80**, 016303 (2009).
[26] Z. Izri, M. N. van der Linden, S. Michelin, and O. Dauchot, Phys. Rev. Lett. **113**, 248302 (2014).
[27] K. V. Kumar, J. S. Bois, F. Jülicher, and S. W. Grill, Phys. Rev. Lett. **112**, 208101 (2014).
[28] H. Masoud and M. J. Shelley, Phys. Rev. Lett. **112**, 128304 (2014).
[29] A. Dominguez, P. Malgaretti, M. N. Popescu, and S. Dietrich, Phys. Rev. Lett. **116**, 078301 (2016).
[30] H. Kim, F. Boulogne, E. Um, I. Jacobi, E. Button, and H. A. Stone, Phys. Rev. Lett. **116**, 124501 (2016).
[31] M. A. Budroni, L. Rongy, and A. De Wit, Phys. Chem. Chem. Phys. **14**, 14619 (2012).
[32] L. Rongy and A. De Wit, J. Chem. Phys. **124**, 164705 (2006); J. Eng. Math. **59**, 221 (2007).
[33] L. Rongy, A. De Wit, and G. M. Homsy, Phys. Fluids **20**, 072103 (2008).
[34] R. Tiani and L. Rongy, J. Chem. Phys. **145**, 124701 (2016).
[35] R. Guzman and D. A. Vasquez, Eur. Phys. J. Spec. Top. **225**, 2573 (2016).
[36] É. Pópity-Tóth, G. Pótári, I. Erdős, D. Horváth, and Á. Tóth, J. Chem. Phys. **141**, 044719 (2014).
[37] A. Hanna, A. Saul, and K. Showalter, J. Am. Chem. Soc. **104**, 3838 (1982).
[38] See Supplemental Material at http://link.aps.org/supplemental/10.1103/PhysRevLett.121.024501 for cell design, for a movie showing the experimental time evolution of the reactive interface, and for a movie showing the evolution of the reactive interface obtained from simulations.
[39] M. Takeda, H. Ina, and S. Kobayashi, J. Opt. Soc. Am. **72**, 156 (1982).
[40] P. Buchhave, Exp. Therm. Fluid. Sci. **5**, 586 (1992).
[41] I. F. Sbalzarini and P. Koumoutsakos, J. Struct. Biol. **151**, 182 (2005).
[42] *Oscillations and Traveling Waves in Chemical Systems*, edited by R. J. Field and M. Burger (Wiley, New York, 1985).
[43] K. Showalter, in *Kinetics of Nonhomogeneous Processes*, edited by G. R. Freeman (Wiley, New York, 1987).
[44] J. H. Merkin and H. Ševčíková, Phys. Chem. Chem. Phys. **1**, 91 (1999).
[45] A. A. Nepomnyashchy, M. G. Velarde, and P. Colinet, *Interfacial Phenomena and Convection* (Chapman and Hall, Boca Raton 2002).